

Post-treatment Control of HIV and Effects of Reversing Exhaustion

Alan S. Perelson, PhD

Theoretical Biology & Biophysics
Los Alamos National Laboratory
Los Alamos, NM

Collaborators

- Youfang Cao – LANL
- Jessica Conway – Penn State

HIV Functional Cure



PRESSWIRE

General Hospital Reveals Fourteen Years of HIV Functional Cure: The Case of the 'Toulon Patient'

A man infected by HIV-1 in 1998 was treated at the time of acute infection with 4 antiretrovirals during 2 years and is now still in remission.

TOULON, VAR, FRANCE, August 5, 2014

A large, 3D, grey block-letter graphic of the word 'CURE' with a slight shadow, set against a white background with a thin grey border.

Modeling Post-treatment Control (PTC)

OPEN ACCESS Freely available online

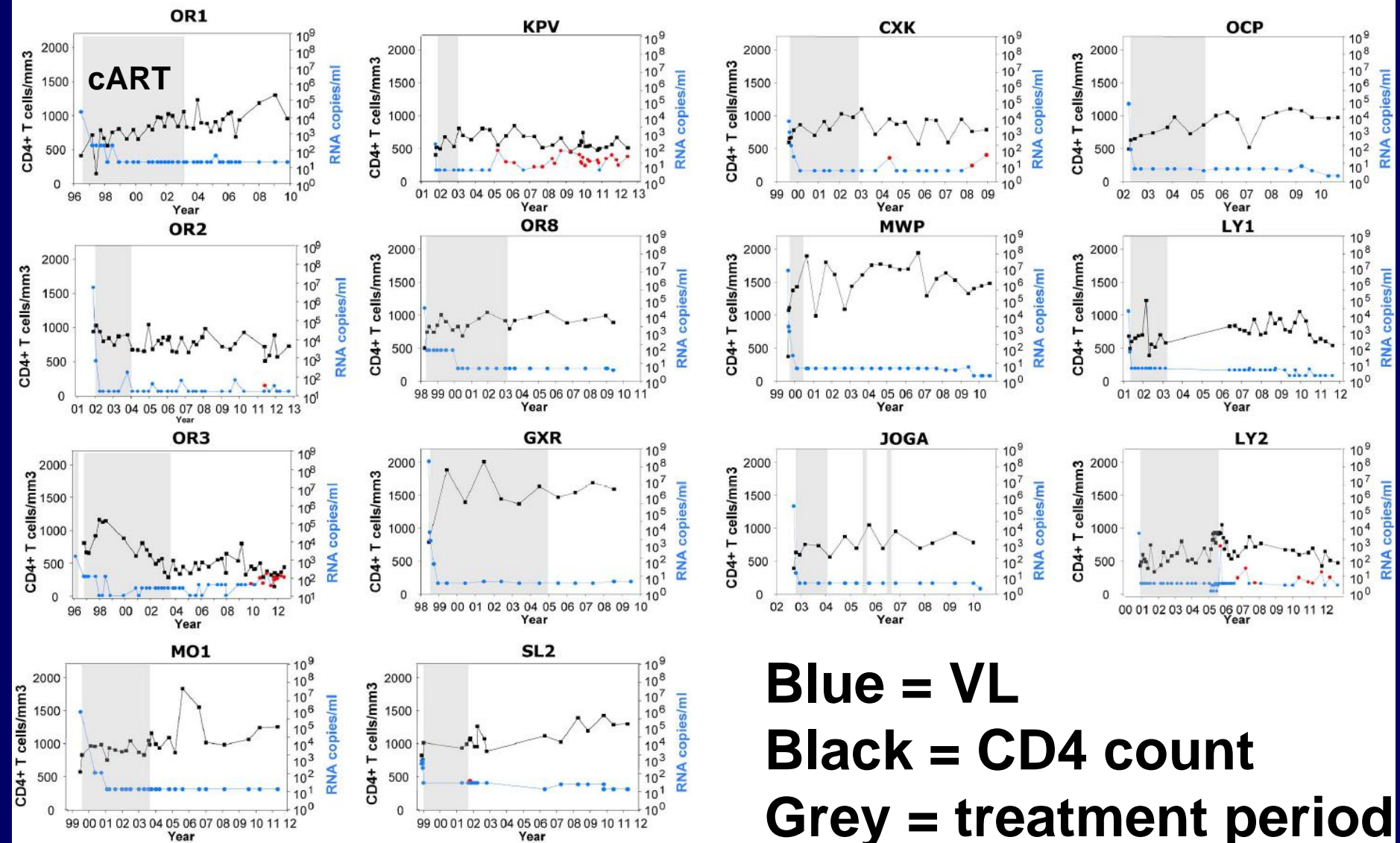
 **PLOS** | PATHOGENS

Post-Treatment HIV-1 Controllers with a Long-Term Virological Remission after the Interruption of Early Initiated Antiretroviral Therapy ANRS VISCONTI Study

Asier Sáez-Cirión^{1*}, Charline Bacchus², Laurent Hocqueloux³, Véronique Avettand-Fenoel^{4,5}, Isabelle Girault⁶, Camille Lecuroux⁶, Valerie Potard^{7,8}, Pierre Versmisse¹, Adeline Melard⁴, Thierry Prazuck³, Benjamin Descours², Julien Guernon², Jean-Paul Viard^{5,9}, Faroudy Boufassa¹⁰, Olivier Lambotte^{6,11}, Cécile Goujard^{10,11}, Laurence Meyer^{10,12}, Dominique Costagliola^{7,8,13}, Alain Venet⁶, Gianfranco Pancino¹, Brigitte Autran², Christine Rouzioux^{4,5*}, the ANRS VISCONTI Study Group[¶]

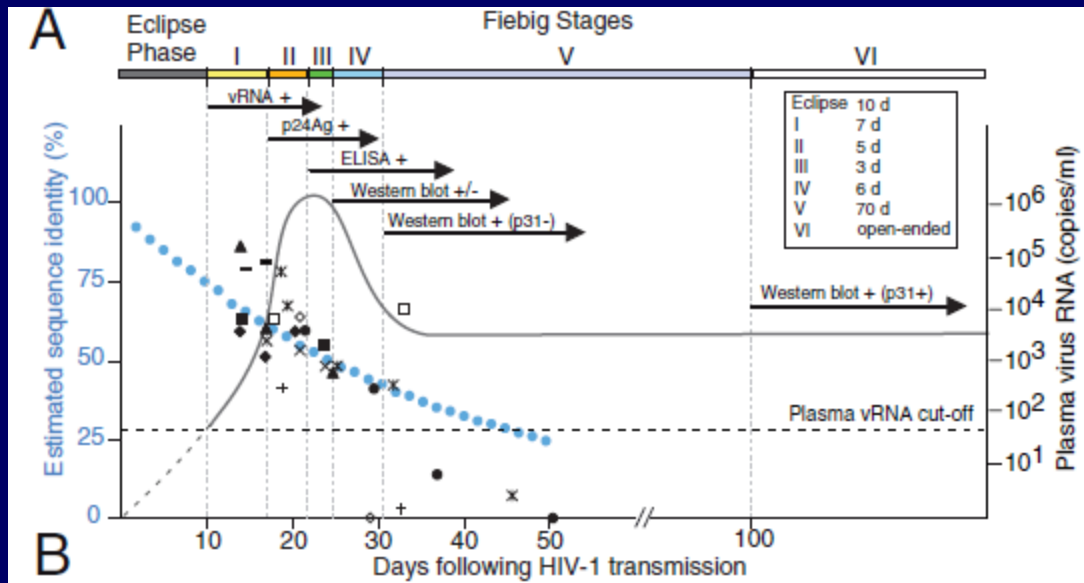
Plos Path 9, e1003211 (2013)

14 subjects were PTCs



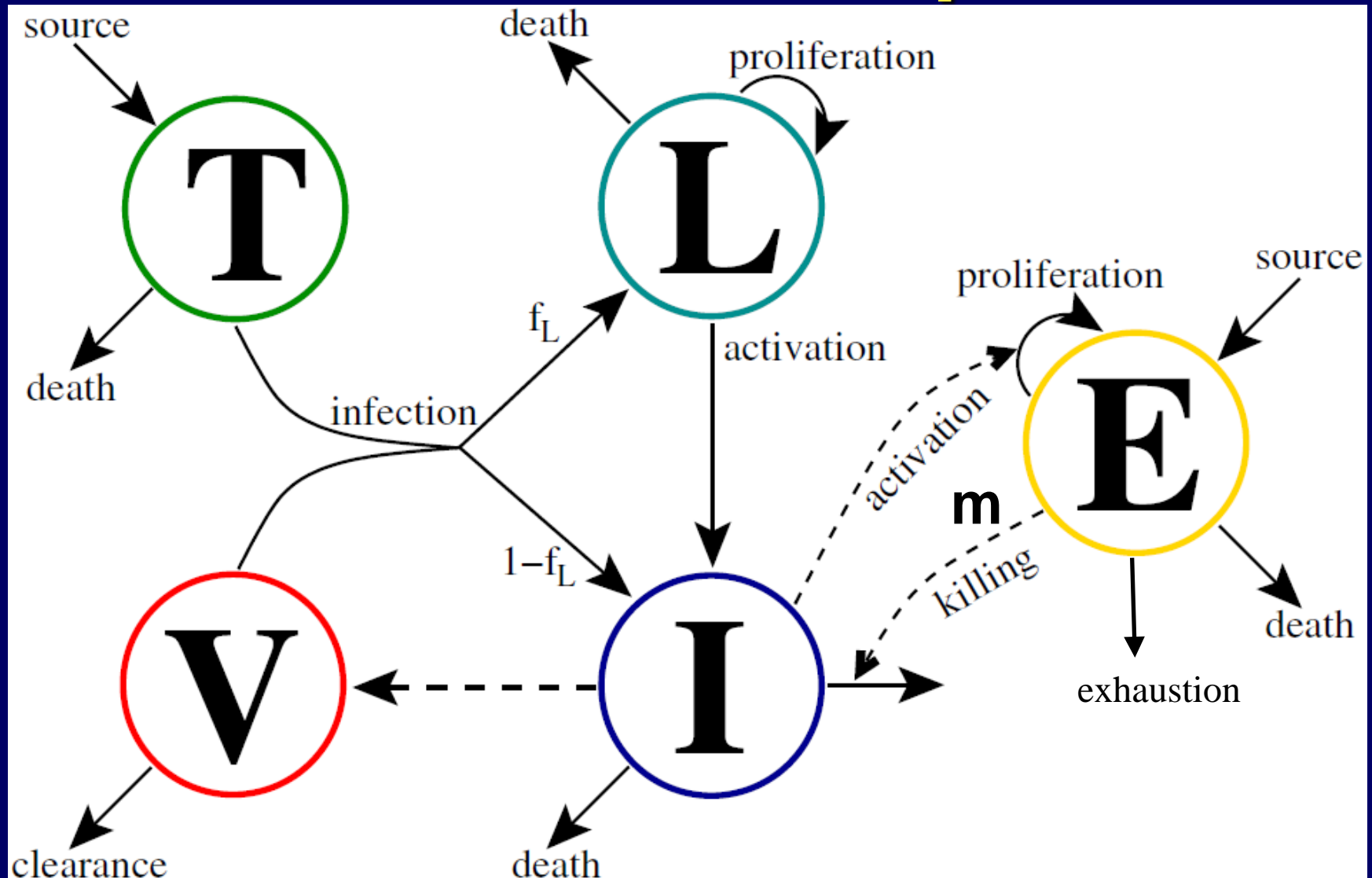
PTCs have two set-points

- Pre-treatment average baseline viral load was 10^5 copies/ml and pts in Fiebig stage V

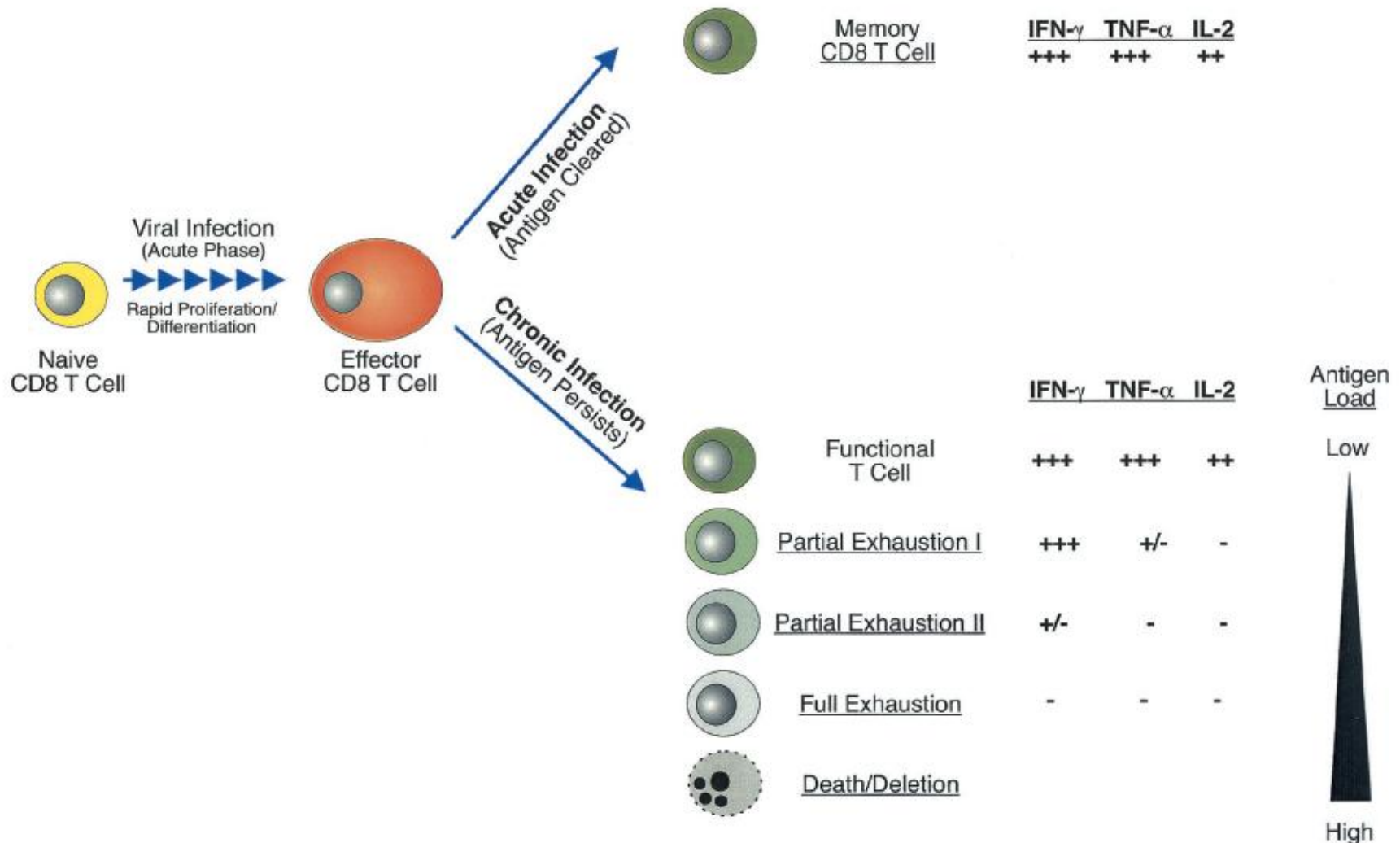


- Post-treatment controllers, VL < 50 copies/ml. VL < 50 /ml is stable for yrs = new set-point, i.e. bistability

Model with 2 set-points



Immune Exhaustion



Wherry et al J Virol 77: 4911 (2003)

Model equations

Target cells, T

Latently infected, L

Productively infected, I

Virus, V

Effector cells, E

$$\begin{aligned}\frac{dT}{dt} &= \lambda - dT - (1 - \epsilon)kVT \\ \frac{dL}{dt} &= \alpha_L(1 - \epsilon)kVT + (\rho - a - d_L)L \\ \frac{dI}{dt} &= (1 - \alpha_L)(1 - \epsilon)kVT - \delta I + aL - mEI \\ \frac{dV}{dt} &= pI - cV \\ \frac{dE}{dt} &= \lambda_E + b_E \frac{I}{K_B + I} E - d_E \frac{I}{K_D + I} E - \mu E.\end{aligned}$$

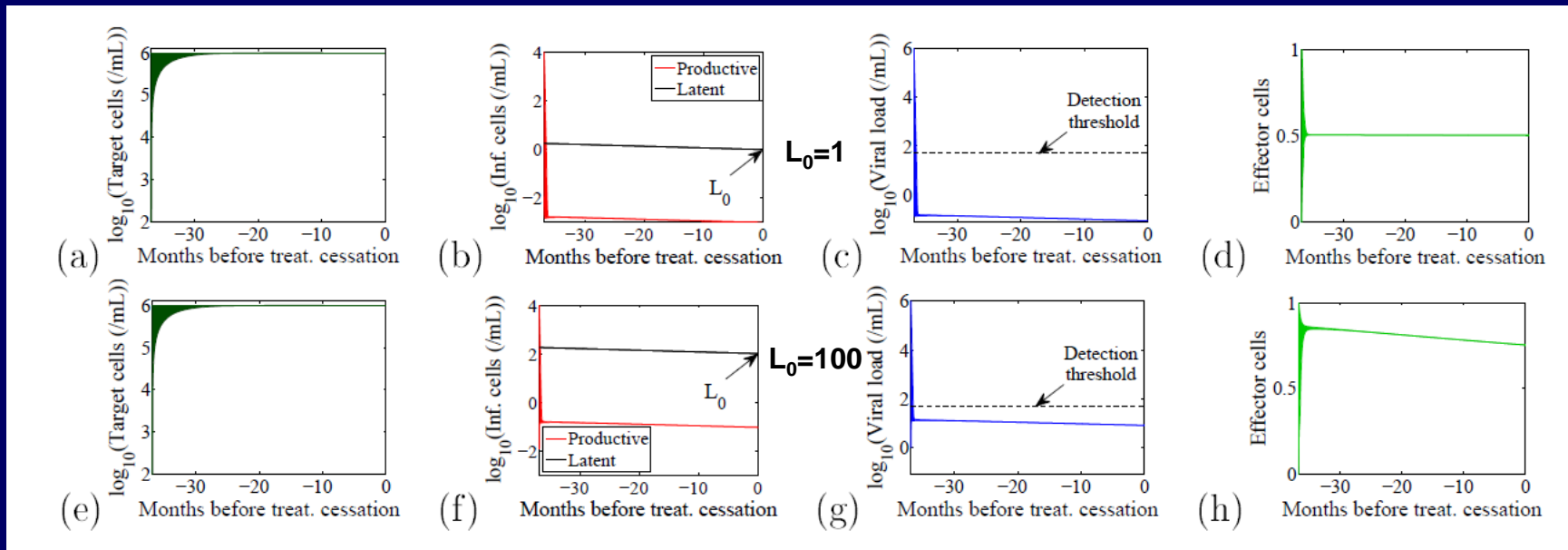
Rate of killing of infected cells by effector cells
= mE (should be $< 1 d^{-1}$)

Have scaled effector cell levels so $0 \leq m \leq 1$.

Details

- Pre-therapy patient has high VL (varies)
- In model, treat with ART, VL decreases to < 50 cp/ml, latently infected cells decrease to low level, L_0 , e.g. $1 - 100 / 10^6$ cells. Exact level is expected to vary among pts due to initial level, treatment length and treatment efficacy.
- After ART stopped, residual viremia and activation of latently infected cells either drives viral rebound or immune system controls.

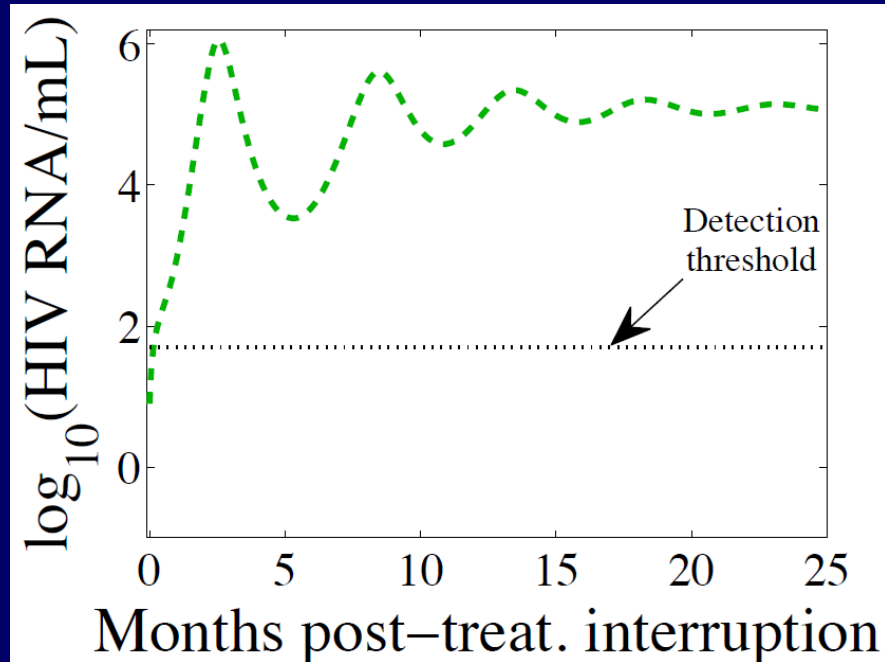
Initial conditions determined by post-treatment L_0



Start with a range of initial conditions – but trajectories quickly establish QSS with $L(t)$

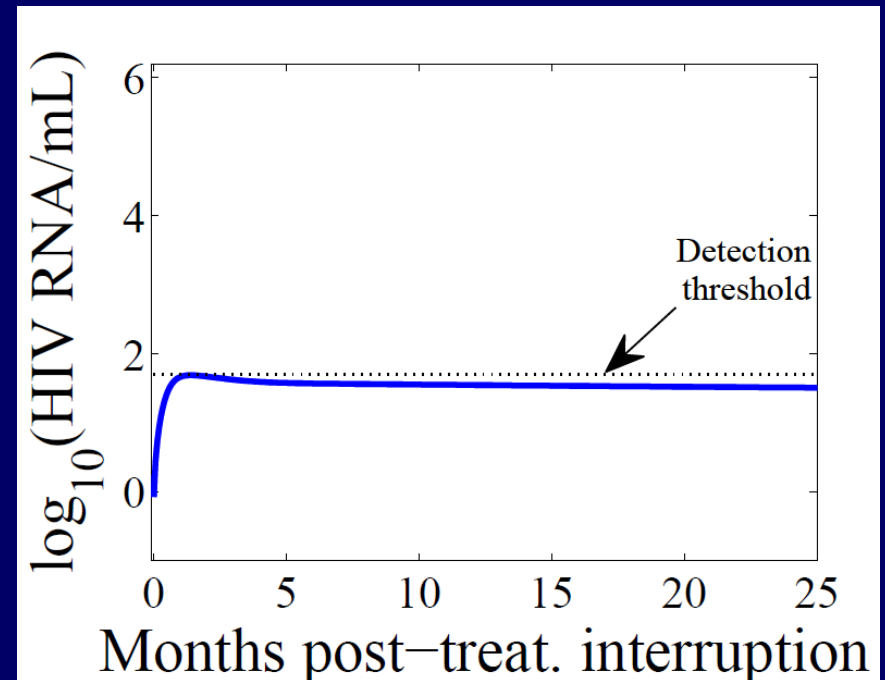
Post-treatment predictions

$L_0 = 100$ per 10^6 cells; $m = 0.32$



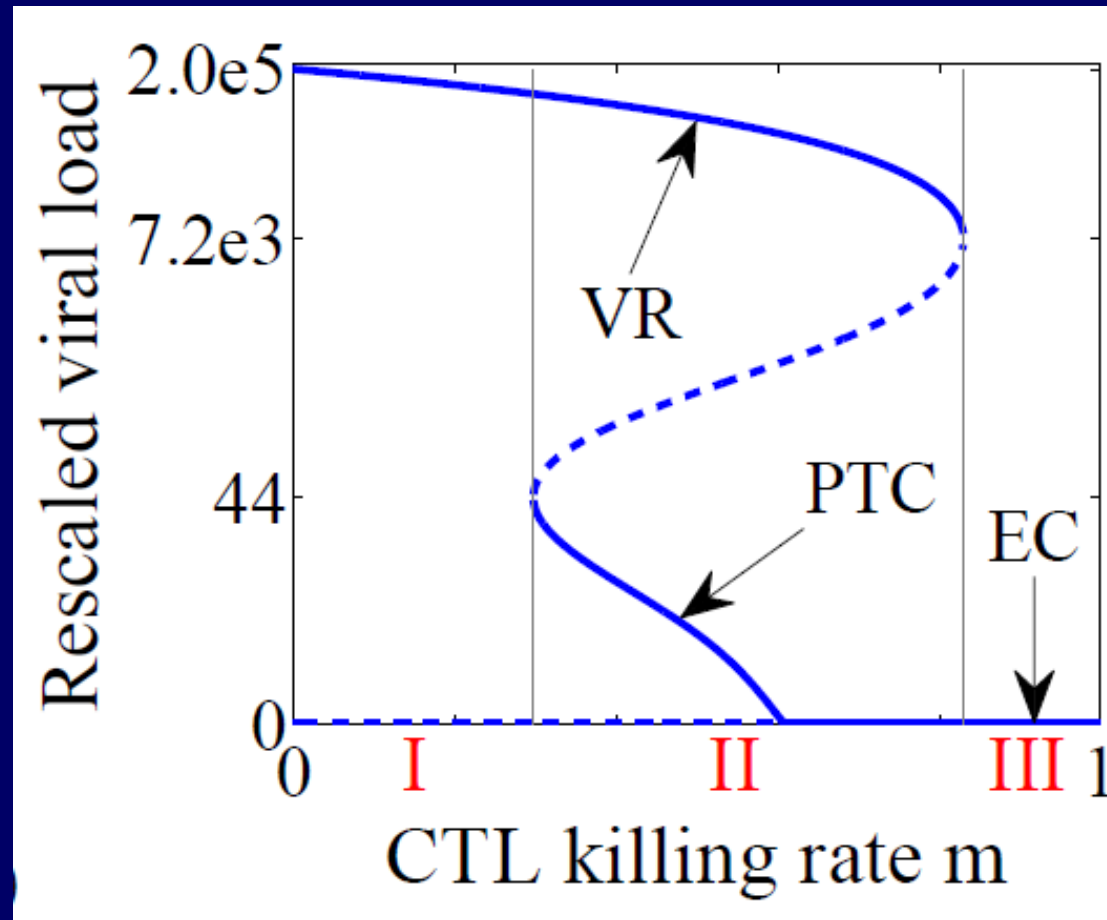
Rebound

$L_0 = 1$ per 10^6 cells; $m = 0.32$



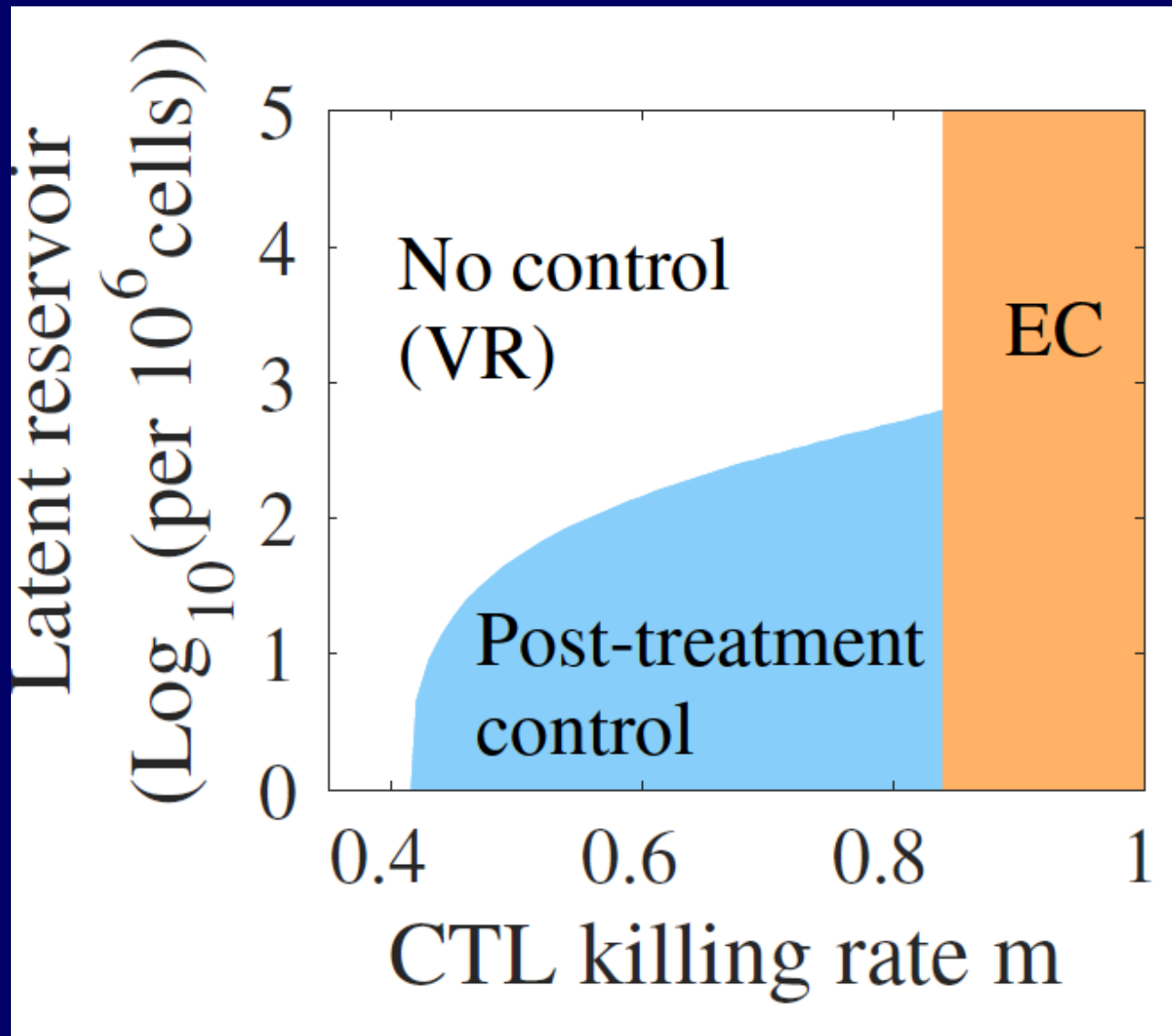
PTC

Post-treatment control (PTC) also depends on strength of immune response



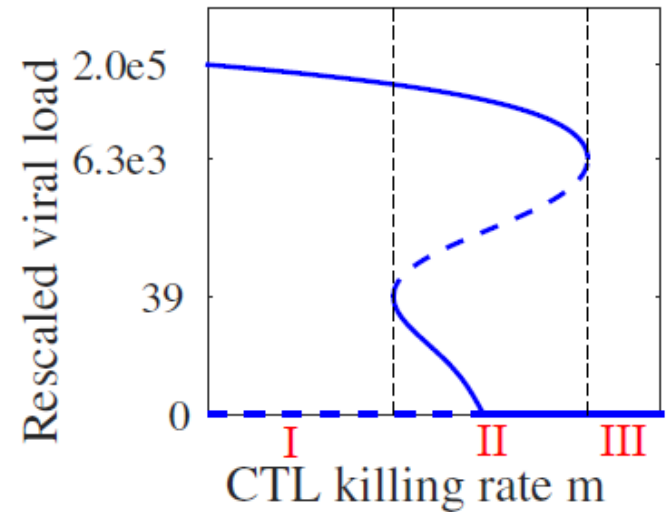
Y-axis is predicted post-treatment set-point VL
(Rescaled with \sinh^{-1})

PTC depends on L_0 and m



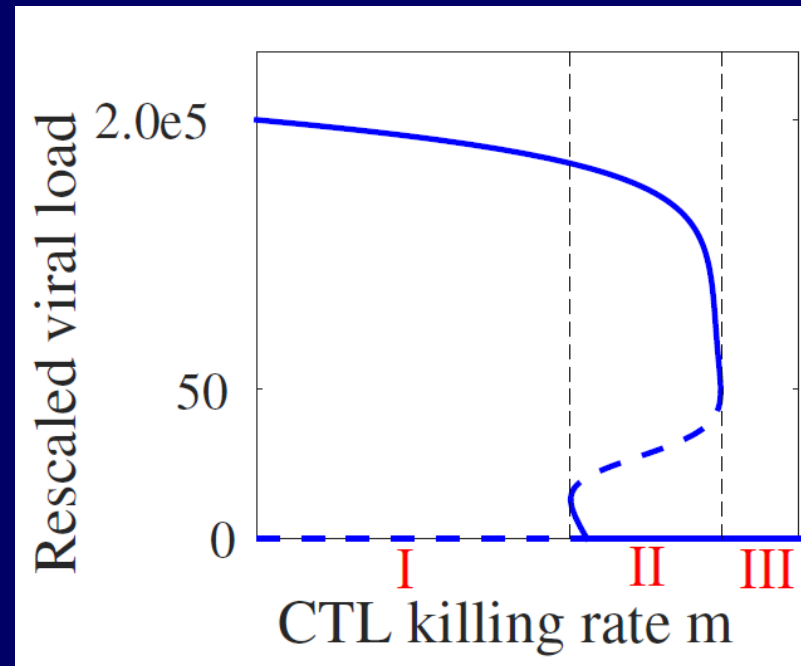
Alternative Models

$$\begin{aligned}
 \frac{dT}{dt} &= \lambda - dT - (1 - \varepsilon)\beta VT \\
 \frac{dL}{dt} &= \alpha_L(1 - \varepsilon)\beta VT - (a + d_L)L + rL \left(1 - \frac{L}{L_{\max}}\right) \\
 \frac{dI}{dt} &= (1 - \alpha_L)(1 - \varepsilon)\beta VT - \delta I + aL - mEI \\
 \frac{dV}{dt} &= pI - cV \\
 \frac{dE}{dt} &= \lambda_E + b_E \frac{I}{K_B + I} E - d_E \frac{I}{K_D + I} E - \mu E.
 \end{aligned}$$

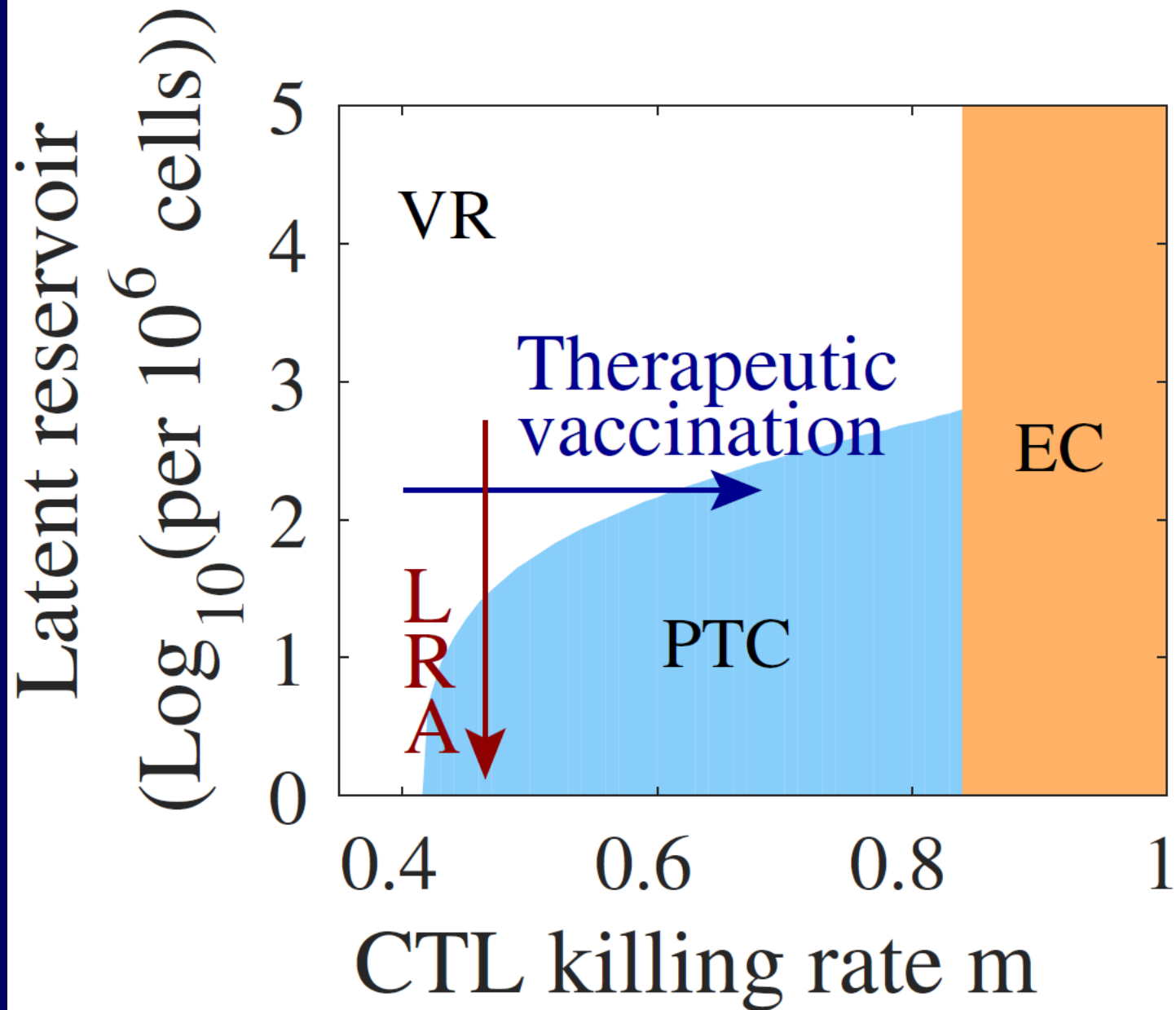


Alternative Exhaustion Model

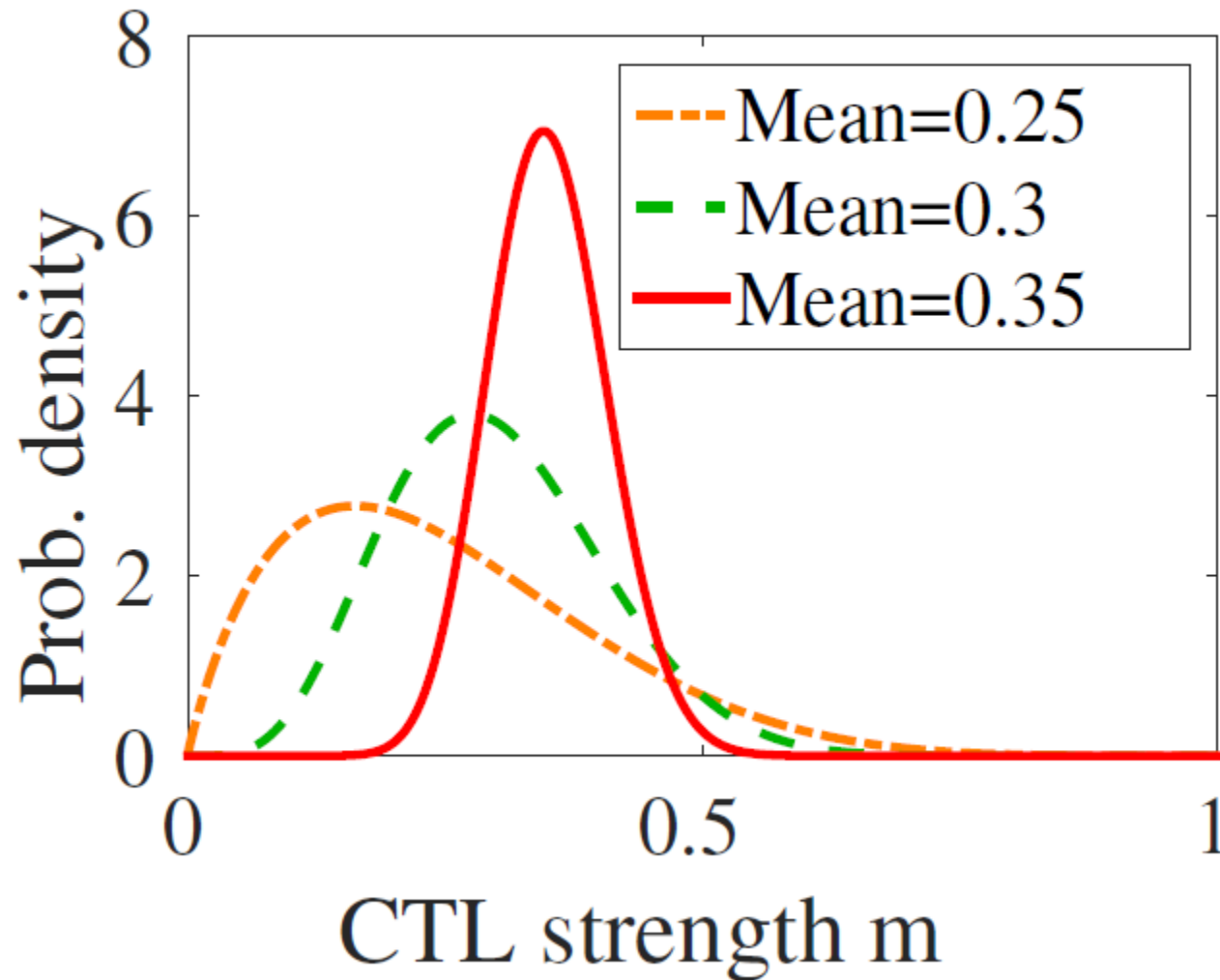
$$\begin{aligned}
 \frac{dT}{dt} &= \lambda - dT - \beta TV \\
 \frac{dL}{dt} &= \alpha_L(1 - \varepsilon)\beta VT + (\rho - a - d_L)L \\
 \frac{dI}{dt} &= (1 - \alpha_L)(1 - \varepsilon)\beta VT - \delta I + aL - mEI \\
 \frac{dV}{dt} &= pI - cV \\
 \frac{dE}{dt} &= \lambda_E + s \frac{I}{\phi + I} E - \xi \frac{Q^n}{q_c^n + Q^n} E - \mu E \\
 \frac{dQ}{dt} &= \kappa \frac{I}{\phi + I} - d_q Q.
 \end{aligned}$$



Q=level of exhaustion; Johnson et al. J Virol. 2011



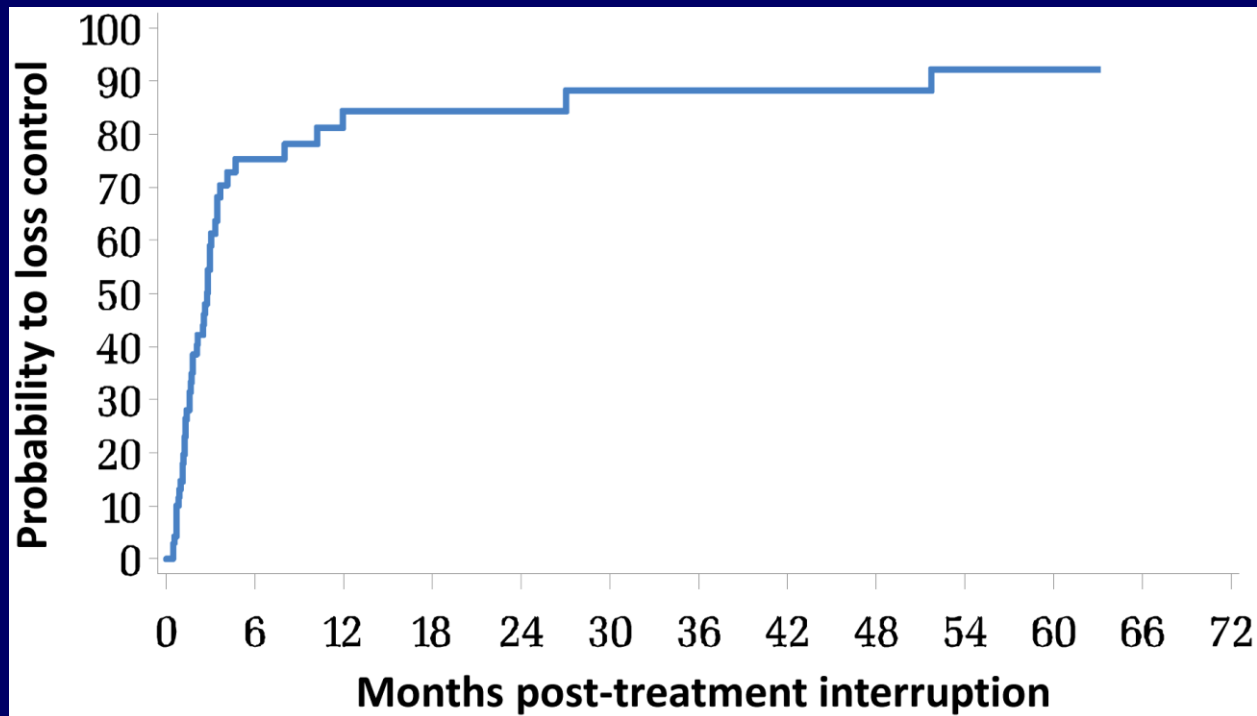
Possible CTL strength distributions



(b)

Viral rebound

- Of the >100 study subjects in the Visconti study only 14 were PTCs; in the remaining the VL rebounded but not immediately. Time to rebound reported for a different French acute infection cohort.

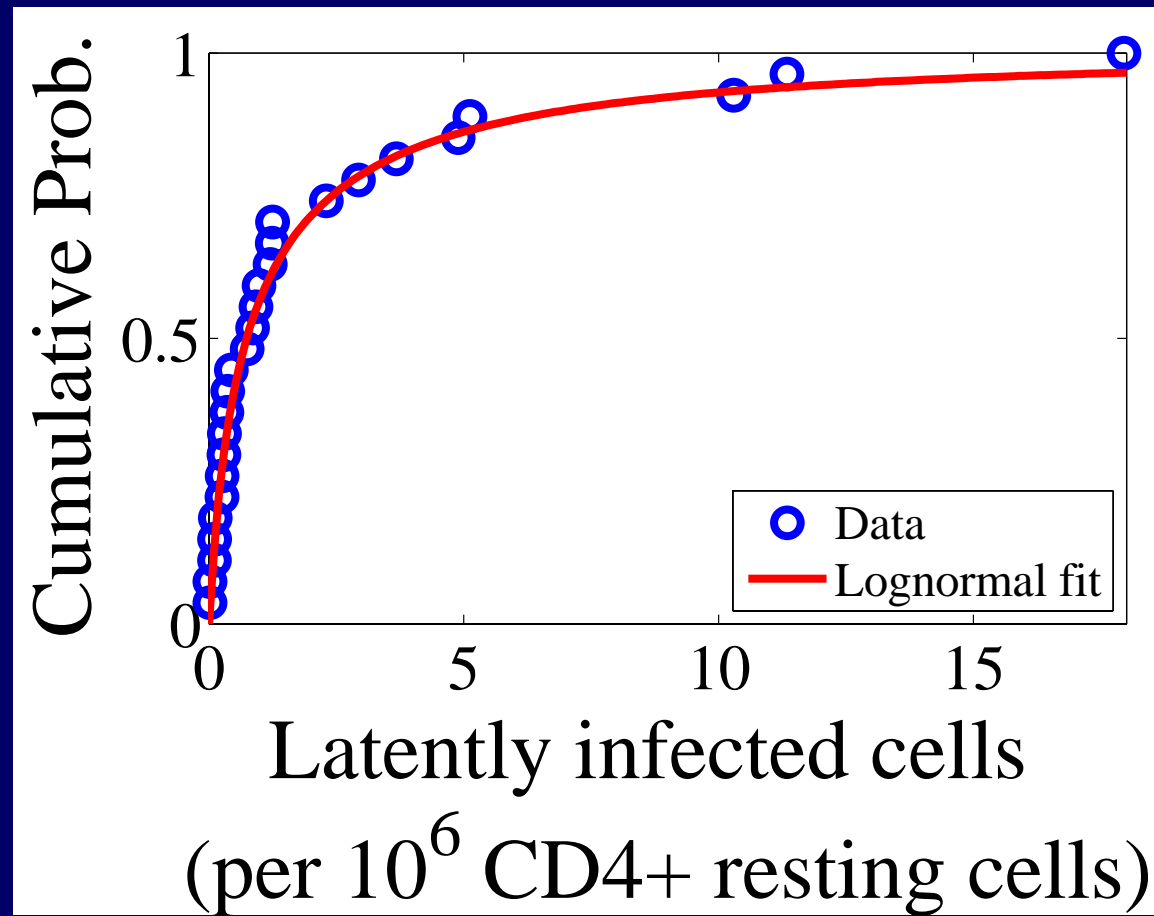


N=74; at least 1 yr ART initiated within 6 mo of infection; loss of control VL > 50/ml

Time to rebound

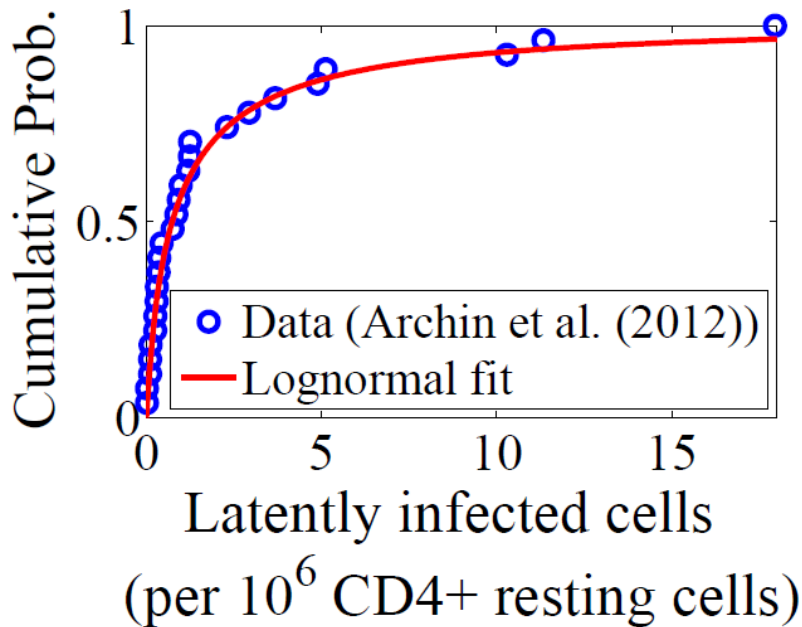
- In our model time to rebound depends on latent reservoir size, L_0 .
- Do not know distribution of latent reservoir sizes in Visconti pts, but in Archin et al. PNAS 2012 reservoir sizes measured after 1 yr of ART in 27 pts treated within 45 days of infection.

Archin et al. PNAS 2012 data fits a lognormal distribution

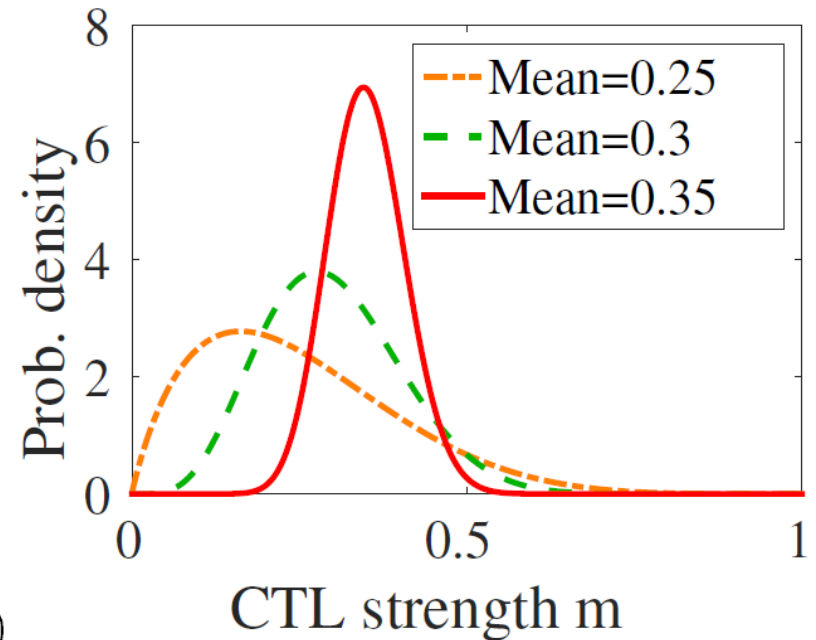


Pts put on therapy ~ 45 d after infection, treated ~ 1 yr

Rebound time depends on latent reservoir size and CTL strength distributions

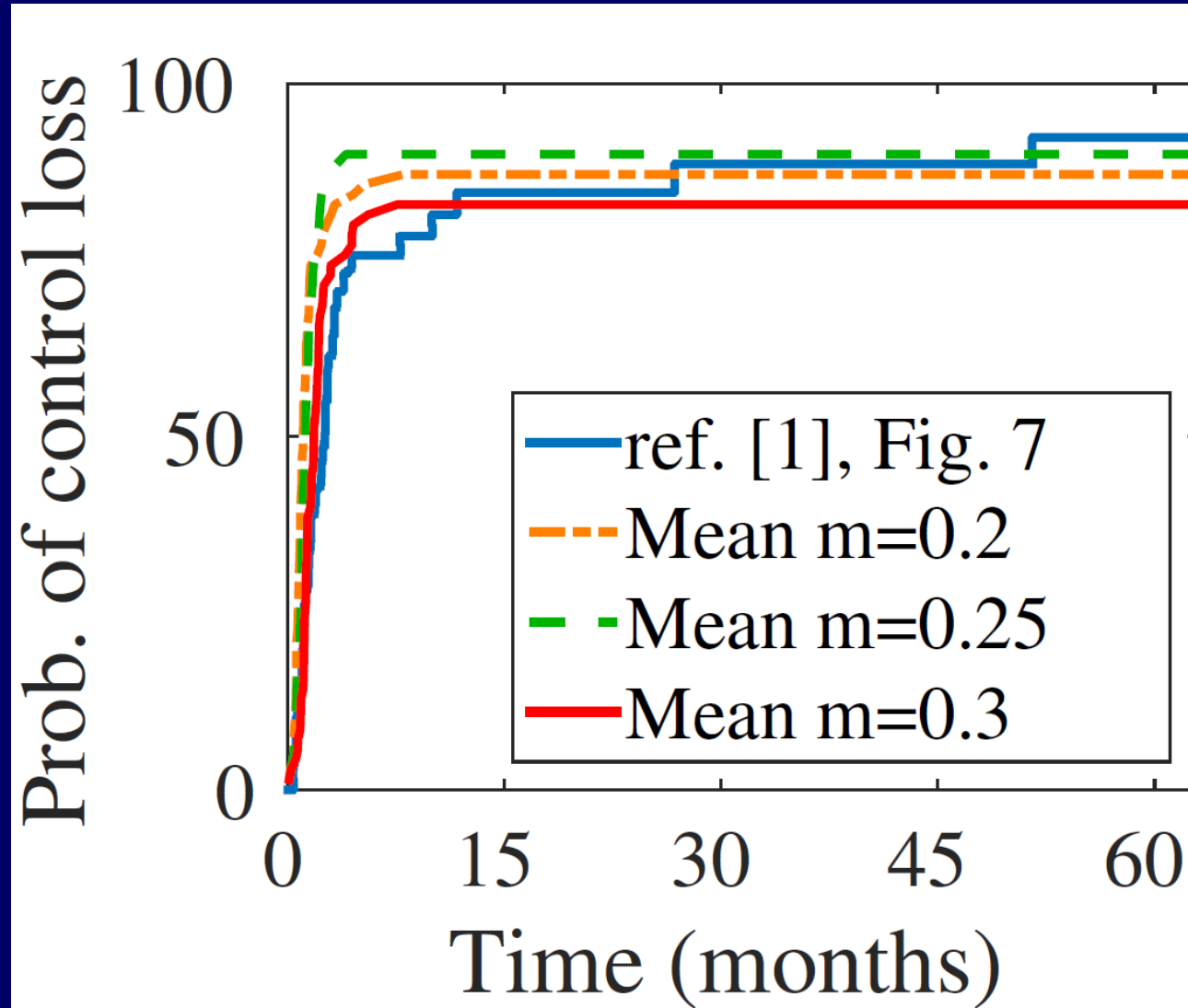


(a)

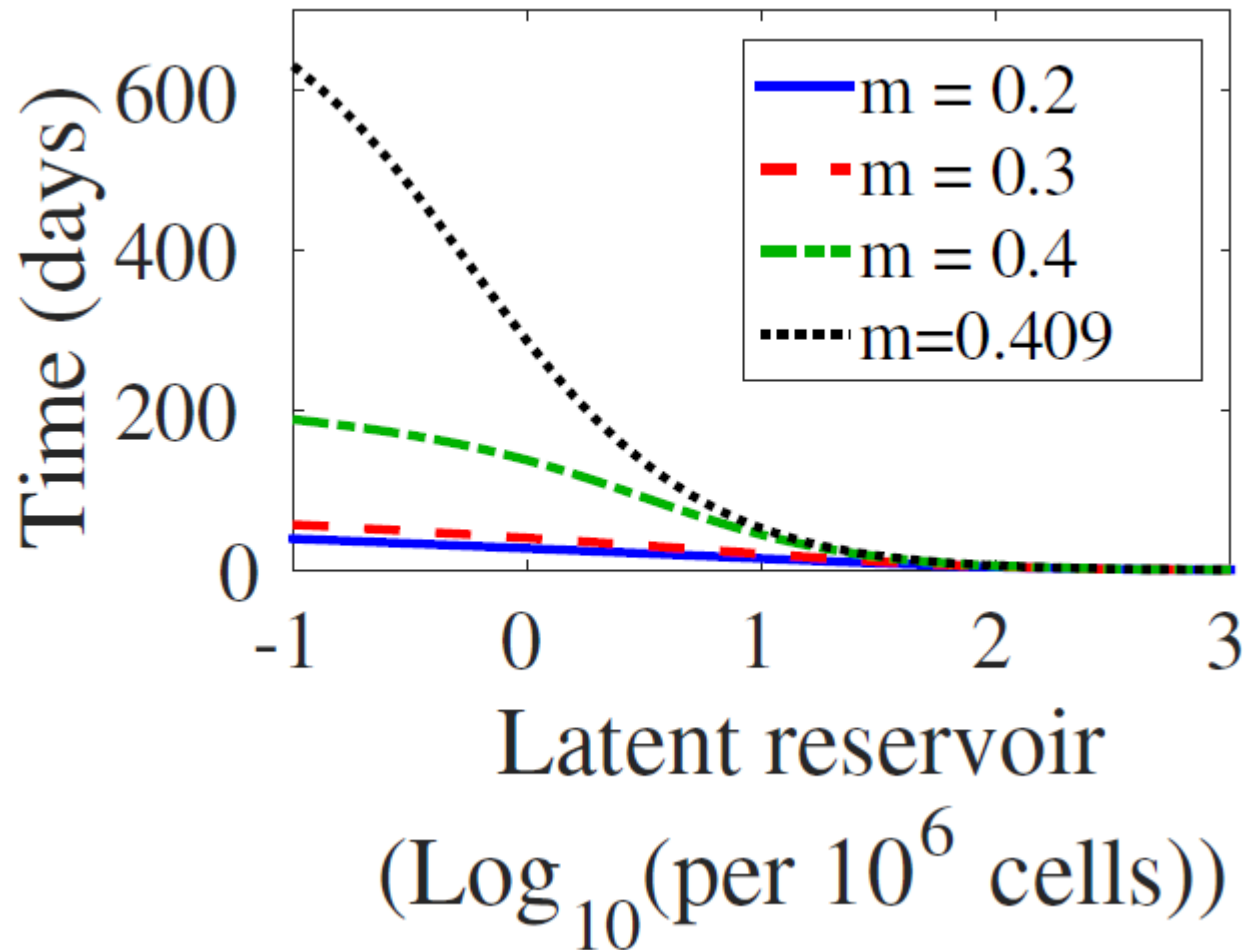


(b)

Model also predicts viral rebound time when there is no control



Rebound time can be quite long, e.g., Mississippi baby



Immune Exhaustion

- Remove effector cell exhaustion model
not longer exhibits bistability – lose
cubic
- Question: Is immune exhaustion
important for post-treatment control?

Overcoming T cell exhaustion in infection and cancer

Kristen E. Pauken and E. John Wherry

Institute for Immunology and Department of Microbiology, University of Pennsylvania Perelman School of Medicine, 421 Curie Blvd, Philadelphia, PA 19104, USA

Inhibitors of the Programmed Cell Death 1: Programmed Cell Death 1 ligand 1 (PD-1:PD-L1) pathway, a central regulator of T cell exhaustion, have been recently shown to be effective for treatment of different cancers. However, clinical responses are mixed, highlighting the need to better understand the mechanisms of action of PD-1:PD-L1, the role of this pathway in immunity to different tumors, and the molecular and cellular effects of PD-1 blockade. Here, we review the molecular regulation of T cell exhaustion, placing recent findings on PD-1 blockade therapies in cancer in the context of the broader understanding of the roles of the PD-1:PD-L1 pathway in T cell exhaustion during chronic infection. We discuss the current understanding of the mechanisms involved in reversing T cell exhaustion, and outline critical areas of focus for future research, both basic and clinical.

cells, which are protected by mechanisms that have evolved to prevent recognition of self, including central tolerance, ignorance or failure to become activated in the periphery, T cell extrinsic regulation [e.g., regulatory T cells, myeloid-derived suppressor cells, suppressive cytokines, such as interleukin (IL)-10, etc.], and T cell intrinsic dysfunction upon inappropriate or excessive antigen stimulation (anergy and exhaustion) [15,17–19]. Antibodies targeting inhibitory pathways including CTLA-4 and PD-1 are paving the way for a new generation of cancer treatment approaches. These ‘checkpoint blockade’ strategies aim to relieve regulatory mechanisms that restrain tumor-infiltrating T cells (TILs) [14,16,20]. The first of these antibodies to gain US FDA approval were ipilimumab in 2011 (anti-CTLA-4, Yervoy, Bristol-Myers Squibb), pembrolizumab in 2014 (anti-PD-1, Keytruda, Merck and Co.), and nivolumab in 2014 (anti-PD-1, Opdivo, Bristol-Myers Squibb), and have all demonstrated

LETTERS

Enhancing SIV-specific immunity *in vivo* by PD-1 blockade

Vijayakumar Velu^{1,2*}, Kehmia Titanji^{1,2*}, Baogong Zhu^{3,4}, Sajid Husain^{1,2}, Annette Pladevega^{1,2}, Lilin Lai^{1,2}, Thomas H. Vanderford⁵, Lakshmi Chennareddi^{1,2}, Guido Silvestri⁵, Gordon J. Freeman^{3,4}, Rafi Ahmed¹ & Rama Rao Amara^{1,2}

Chronic immunodeficiency virus infections are characterized by dysfunctional cellular and humoral antiviral immune responses^{1–3}. As such, immune modulatory therapies that enhance and/or restore the function of virus-specific immunity may protect from disease progression. Here we investigate the safety and immune restoration potential of blockade of the co-inhibitory receptor programmed death 1 (PD-1)^{4,5} during chronic simian immunodeficiency virus (SIV) infection in macaques. We demonstrate that PD-1 blockade using an antibody to PD-1 is well tolerated and results in rapid expansion of virus-specific CD8 T cells with improved functional quality. This enhanced T-cell immunity was seen in the blood and also in the gut, a major reservoir of SIV infection. PD-1 blockade also resulted in proliferation of memory B cells and increases in SIV envelope-specific antibody. These improved immune responses were associated with significant reductions in plasma viral load and also prolonged the survival of SIV-infected macaques. Blockade was effective during the early (week 10) as well as late (~week 90) phases of chronic infection even under conditions of severe lymphopenia. These results demonstrate

PD-1 blockade was performed using an antibody specific to human PD-1 that blocks the interaction between macaque PD-1 and its ligands (PDLs) *in vitro*¹⁵. Blockade was performed during the early (10 weeks) as well as late (~90 weeks) phases of chronic SIV infection. Nine macaques (five during the early phase and four during the late phase) received the anti-PD-1 antibody and five macaques (three during the early phase and two during the late phase) received an isotype control antibody (Synagis, anti-respiratory syncytial virus (RSV)-specific)¹⁷.

PD-1 blockade during chronic SIV infection resulted in a rapid expansion of SIV-specific CD8 T cells in the blood of all macaques (Fig. 1a, b). We were able to study the CD8 T-cell responses to two immunodominant epitopes, Gag CM9 (ref. 18) and Tat SL8/TL8 (ref. 19), using major histocompatibility complex (MHC) I tetrameric complexes in seven of the anti-PD-1-antibody-treated and three of the control-antibody-treated macaques that expressed the Mamu A*01 histocompatibility molecule. Consistent with previous data¹⁵, most (>98%) of the Gag-CM9 tetramer-specific CD8 T cells expressed PD-1 before blockade (data not shown). After PD-1

Model with exhausted cells

$$\frac{dT}{dt} = \lambda - d_T T - (1 - \epsilon)\beta VT$$

$$\frac{dL}{dt} = \alpha_L(1 - \epsilon)\beta VT + (\rho - a - d_L)L$$

$$\frac{dI}{dt} = (1 - \alpha_L)(1 - \epsilon)\beta VT - \delta I + aL - mEI$$

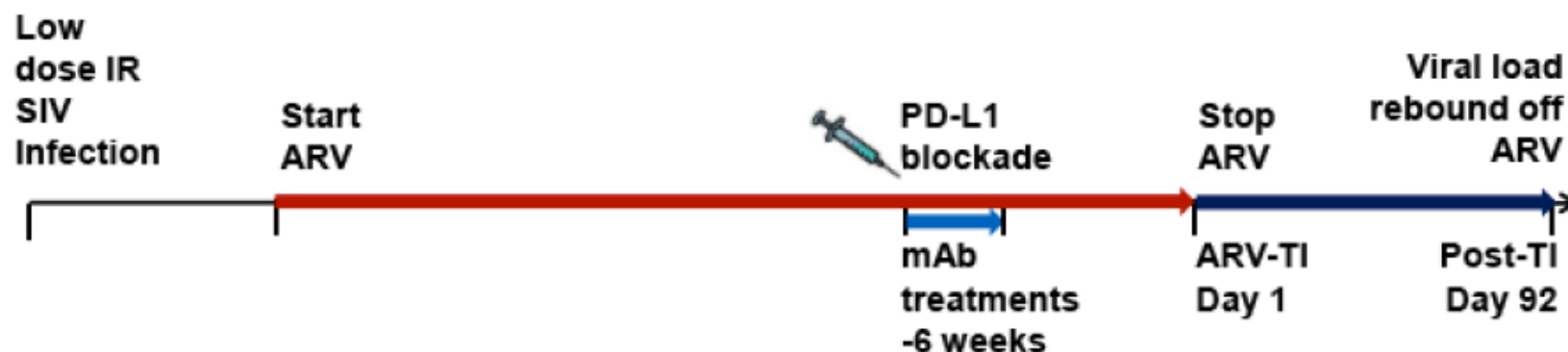
$$\frac{dV}{dt} = pI - cV$$

$$\frac{dE}{dt} = \lambda_E + b_E \frac{I}{K_B + I} E - d_E \frac{I}{K_D + I} E - \mu E + k_{act} \frac{Ab(t)}{EC_{50} + Ab(t)} X$$

$$\frac{dX}{dt} = d_E \frac{I}{K_D + I} E - d_X X - k_{act} \frac{Ab(t)}{EC_{50} + Ab(t)} X$$

**X= exhausted cells, Ab = checkpoint inhibitor Ab
e.g. anti-PD-1 or anti-PD-L1**

Study Overview

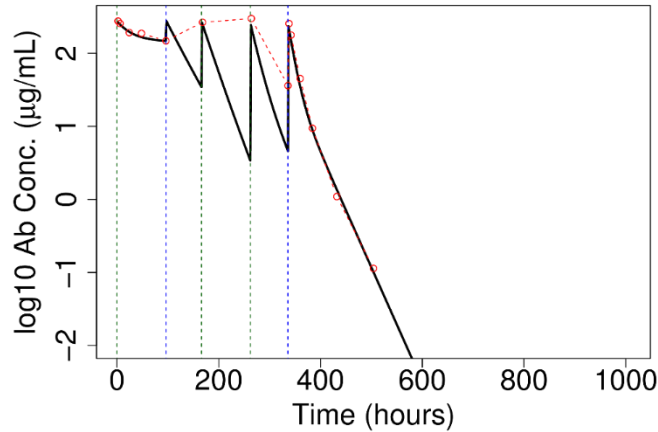


Entry criteria: sustained SIV RNA ≤ 50 copies ml CD4+ > 500 cells/ul

BMS-936559: 5 doses, 10mg/kg over 2 weeks (day 0, 4, 7, 11, 14)

Antibody PK measured-Ab(t) known for each monkey

P294

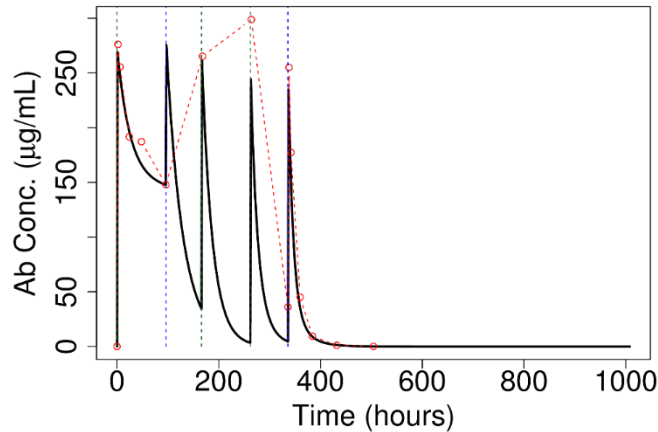


Dose 1: PK1 = $\left(c_1^1 = 152 \frac{\mu\text{g}}{\text{mL}}; c_2^1 = 122 \frac{\mu\text{g}}{\text{mL}}; k_1^1 = 0.0005 \text{ h}^{-1}; k_2^1 = 0.04 \text{ h}^{-1}\right)$

Dose 2: $0.75 \times \text{PK1} + 0.25 \times \text{PK2}$

Dose 3: $0.50 \times \text{PK1} + 0.50 \times \text{PK2}$

Dose 4: $0.25 \times \text{PK1} + 0.75 \times \text{PK2}$



Dose 5: PK2 = $\left(c_1^2 = 215 \frac{\mu\text{g}}{\text{mL}}; c_2^2 = 40 \frac{\mu\text{g}}{\text{mL}}; k_1^2 = 0.1 \text{ h}^{-1}; k_2^2 = 0.036 \text{ h}^{-1}\right)$

Fitting the viral dynamics model parameters from the viral load data

$$\begin{aligned}\frac{dT}{dt} &= \lambda - d_T T - (1 - \epsilon)\beta VT \\ \frac{dL}{dt} &= \alpha_L(1 - \epsilon)\beta VT + (\rho - a - d_L)L \\ \frac{dI}{dt} &= (1 - \alpha_L)(1 - \epsilon)\beta VT - \delta I + aL - mEI \\ \frac{dV}{dt} &= pI - cV \\ \frac{dE}{dt} &= \lambda_E + b_E \frac{I}{K_B + I} E - d_E \frac{I}{K_D + I} E - \mu E + k_{act} \frac{Ab(t)}{EC_{50} + Ab(t)} X \\ \frac{dX}{dt} &= d_E \frac{I}{K_D + I} E - d_X X - k_{act} \frac{Ab(t)}{EC_{50} + Ab(t)} X\end{aligned}$$

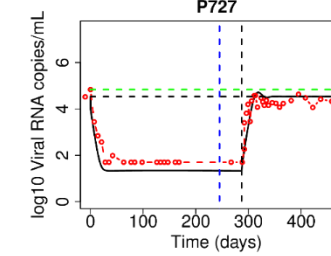
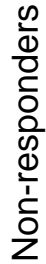
Using fitted PK parameters for the anti-PD-L1 dynamics

$$Ab(t) = c_1 e^{-k_1 t} + c_2 e^{-k_2 t}$$

→ Indicate parameters to fit from data

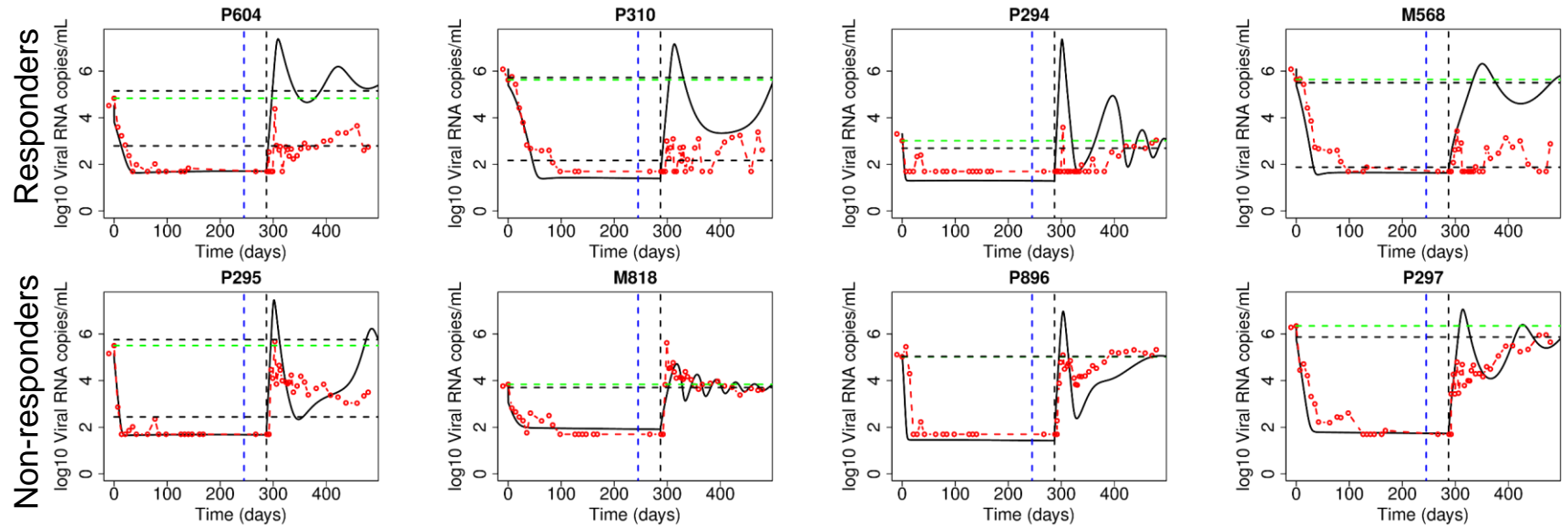
Viral dynamics		
→ λ	1×10^4 cells/mL/day	Target cell production rate
d_T	0.01 /day	Target cell death rate
→ β	1.5×10^{-8} mL/virus/day	Mass-action infectivity
→ δ	1.0 /day	Infected cell death rate
N	3500	Burst size
p	δN	Viral production rate, $p = \delta N$
c	23 /day	Viral clearance rate
ϵ	0.9	Drug efficacy
Latent cell dynamics		
a	1×10^{-3} /day	Latent cell activation rate
d_L	4×10^{-3} /day	Latent cell death rate
ρ	4.5×10^{-3} /day	Latent cell proliferation rate
α_L	1×10^{-6}	Probability of a newly infected cell becomes latent
Effector cell dynamics		
→ m	0.12 μ L/cell/day	Effector cell killing rate
→ λ_E	1.0 cell/ μ L/day	Effector cell basal production rate
→ b_E	1.0 /day	Effector cell activated proliferation coefficient
→ d_E	2.0 /day	Effector cell activated exhaustion coefficient
→ μ	2.0 /day	Effector cell basal death rate
K_B	0.1 cells/mL	Saturation parameter for activated effector cell production
K_D	5.0 cells/mL	Saturation parameter for activated effector cell exhaustion
Exhausted cell dynamics		
k_{act}	1.0 /day	Exhaustion reversal coefficient
EC_{50}	0.04 $\frac{\mu g}{mL}$	
d_X	0.5 μ /day	Exhausted cell death rate

Responders



- Anti-PD-L1
- - - VL data
- - - VL at t_0 in the data
- VL simulations
- - - Steady state VL in the simulation

Simulations using fitted parameters: Removing Ab from treatment group



—○— VL data

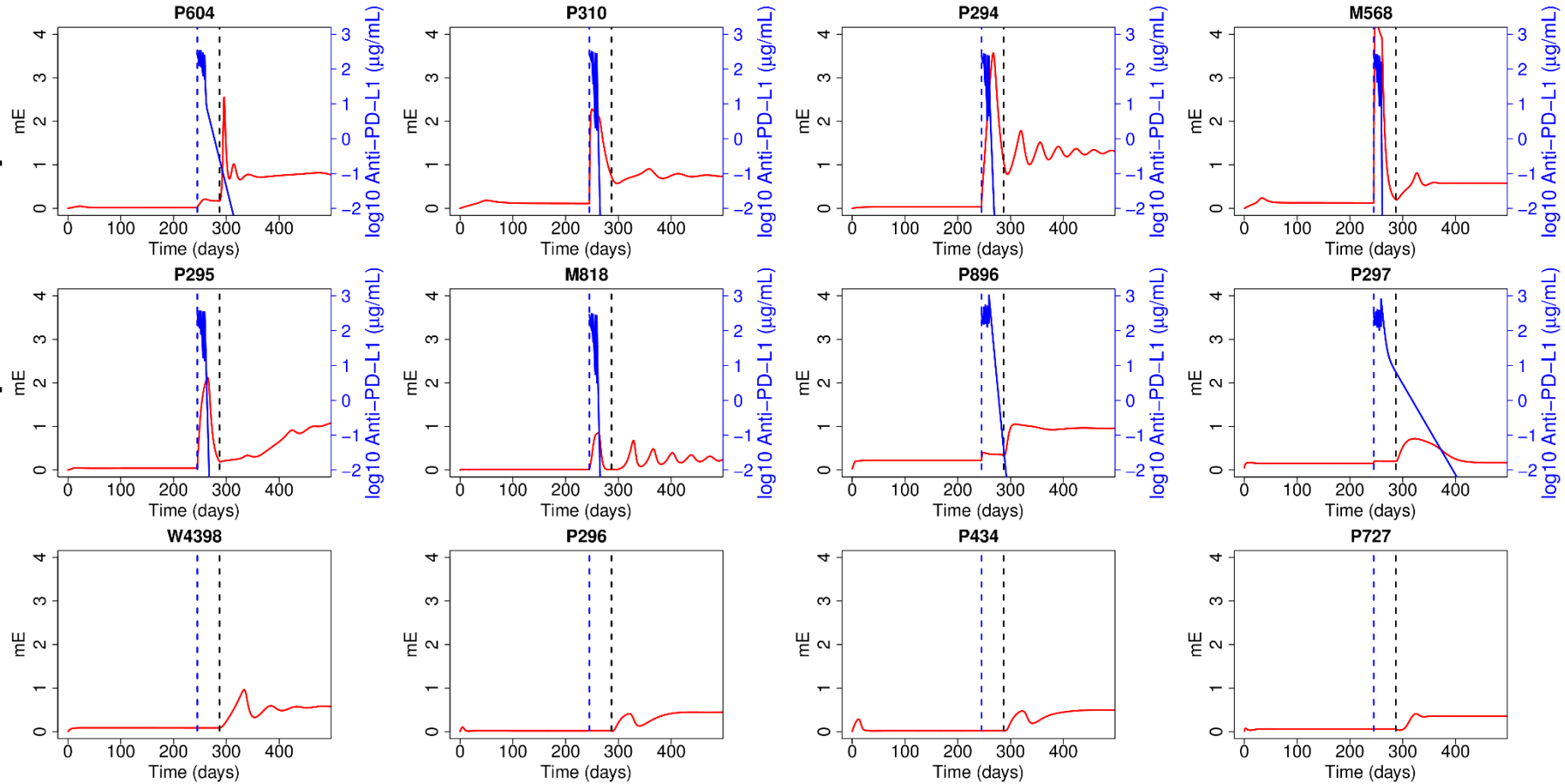
— VL at t_0 in the data

— VL simulations

— Steady state VL in the simulation

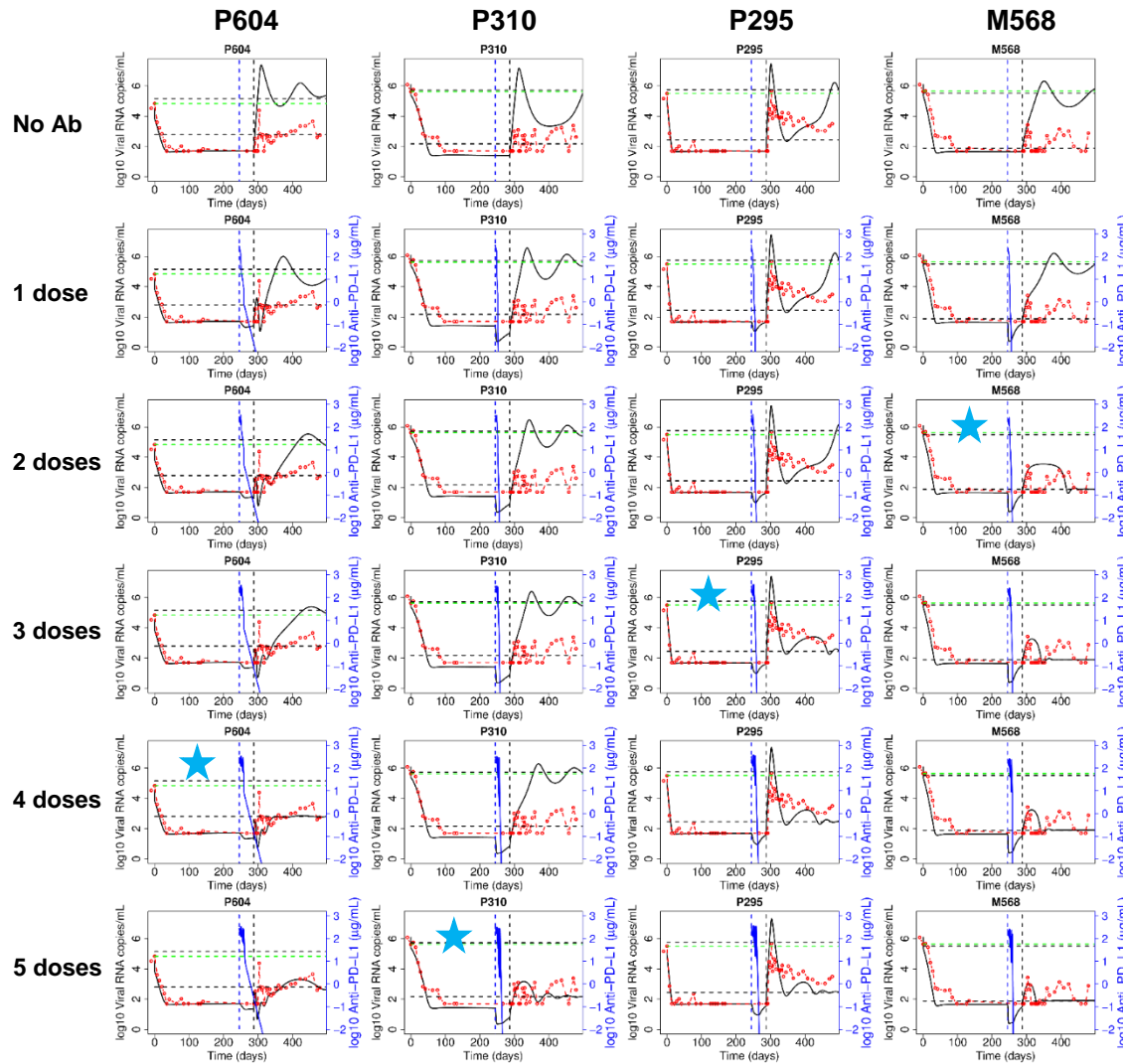
Simulations using fitted parameters: the killing rate of infected cells (mE)

Non-responders
Control



Anti-PD-L1
mE

Fewer doses of Ab for responders



- One dose is not enough to switch the fixed point.
- To move from the high VL fixed point to the low one:
 - M568 needs 2 doses
 - P295 needs 3 doses
 - P604 needs 4 doses
 - P310 needs 5 doses

Model reduction.

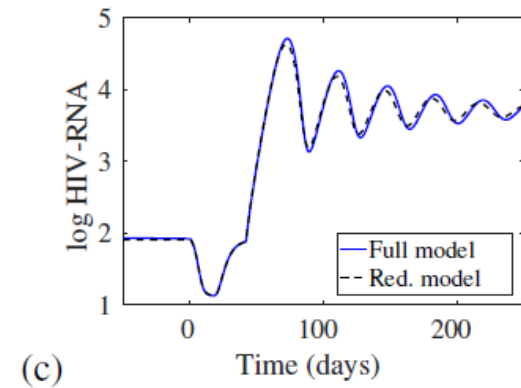
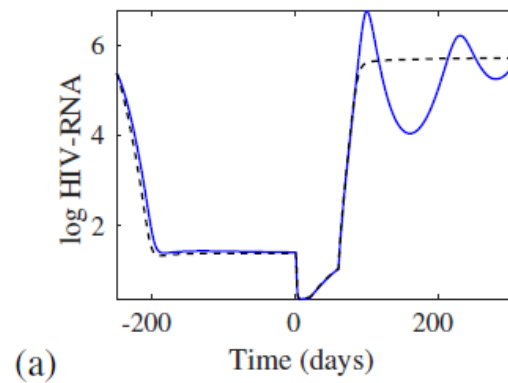
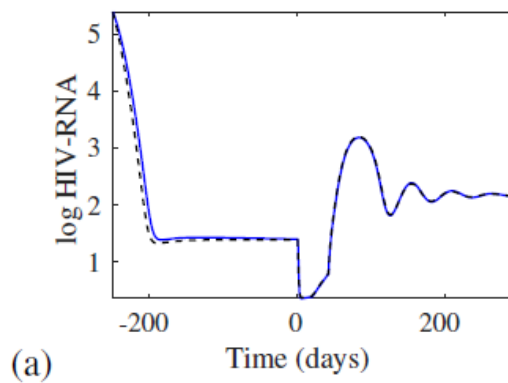
First, use quasi-steady approximation $V = pI/c$

$$\begin{aligned}\dot{T} &= \lambda - d_T T - (1 - \varepsilon)kT pI/c \\ \dot{L} &= \alpha_L(1 - \varepsilon)kT pI/c + (\rho - a - \delta_L)L \\ \dot{I} &= (1 - \alpha_L)(1 - \varepsilon)kT pI/c + aL - \delta I - mEI \\ \dot{E} &= \lambda_E + b_E \frac{IE}{K_b + I} - d_E \frac{IE}{K_d + I} - \mu E + k_{act} \frac{Ab(t)}{EC_{50} + Ab(t)} X \\ \dot{X} &= d_E \frac{IE}{K_d + I} - \mu d_X X - k_{act} \frac{Ab(t)}{EC_{50} + Ab(t)} X\end{aligned}$$

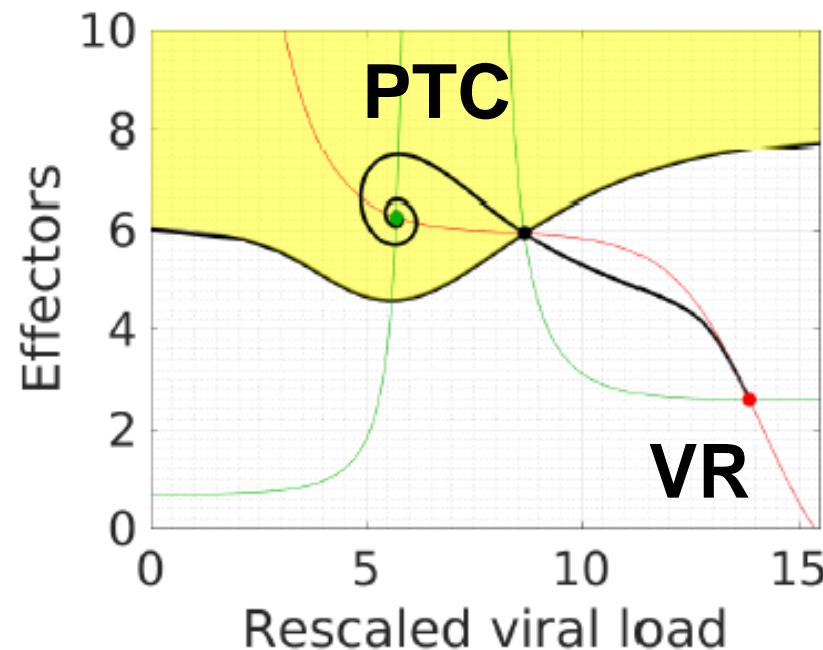
and then (non-traditionally) $T = c\lambda / [cd_T + p(1 - \varepsilon)\beta I]$,

$$\begin{aligned}\dot{L} &= \alpha_L(1 - \varepsilon)kp\lambda I / (cd_T + p(1 - \varepsilon)\beta I) + (\rho - a - \delta_L)L \\ \dot{I} &= (1 - \alpha_L)(1 - \varepsilon)kp\lambda I / (cd_T + p(1 - \varepsilon)\beta I) + aL - \delta I - mEI \\ \dot{E} &= \lambda_E + b_E \frac{IE}{K_b + I} - d_E \frac{IE}{K_d + I} - \mu E + k_{act} \frac{Ab(t)}{EC_{50} + Ab(t)} X\end{aligned}$$

Comparison of Dynamics of reduced and full models



Phase Plane Analysis, P310 parameters with $aL0 = 0.0353$



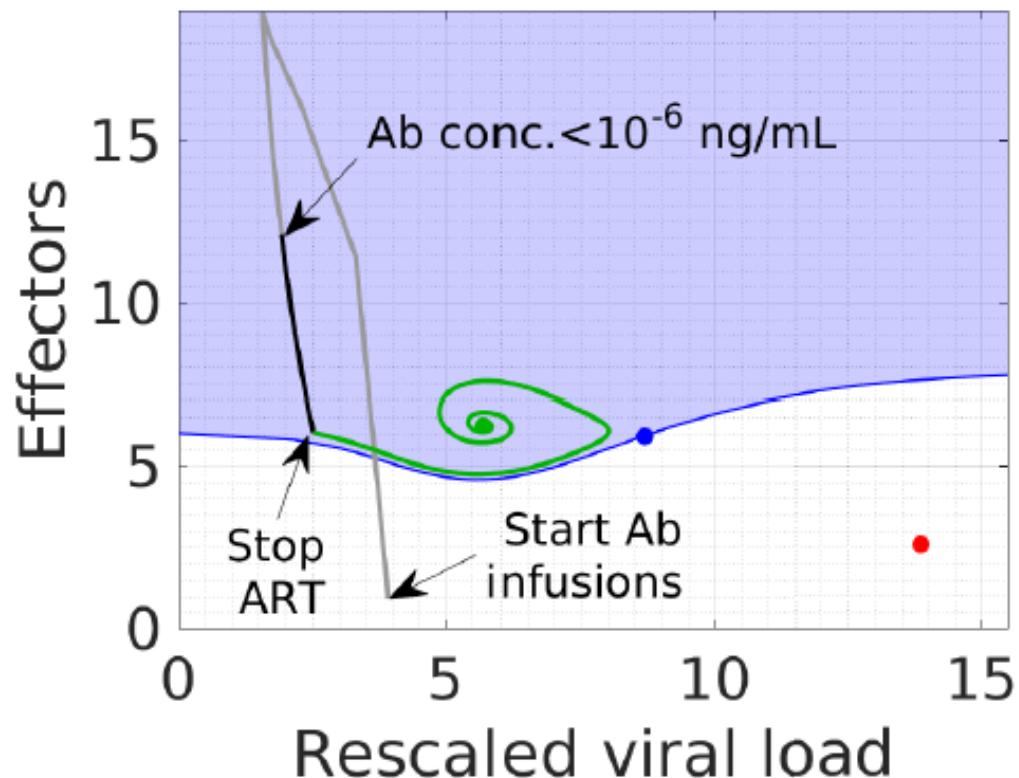
Nullclines: indicated by the green (horizontal) and red (vertical) lines.

Equilibria: green dot is the control, stable state; blue the rebound, stable state; and black the unstable saddle point.

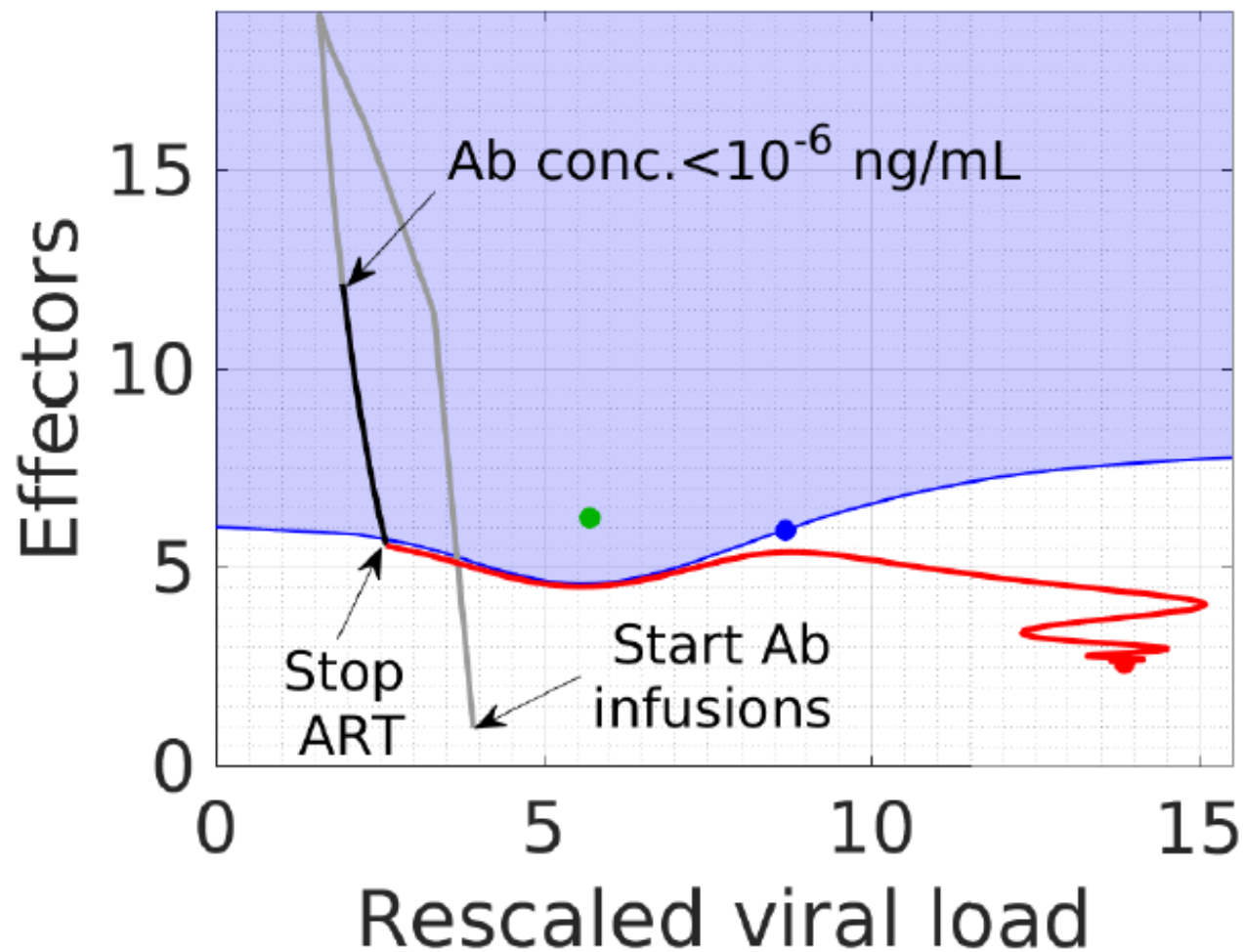
Basin of attraction: Stable manifold of the saddle point forms the boundary of the stable equilibria basin of attraction: yellow = control, white = no control. Unstable manifolds of the saddle point are also included, leading to the control and rebound equilibria respectively.

Full Model Dynamics on Phase Plane

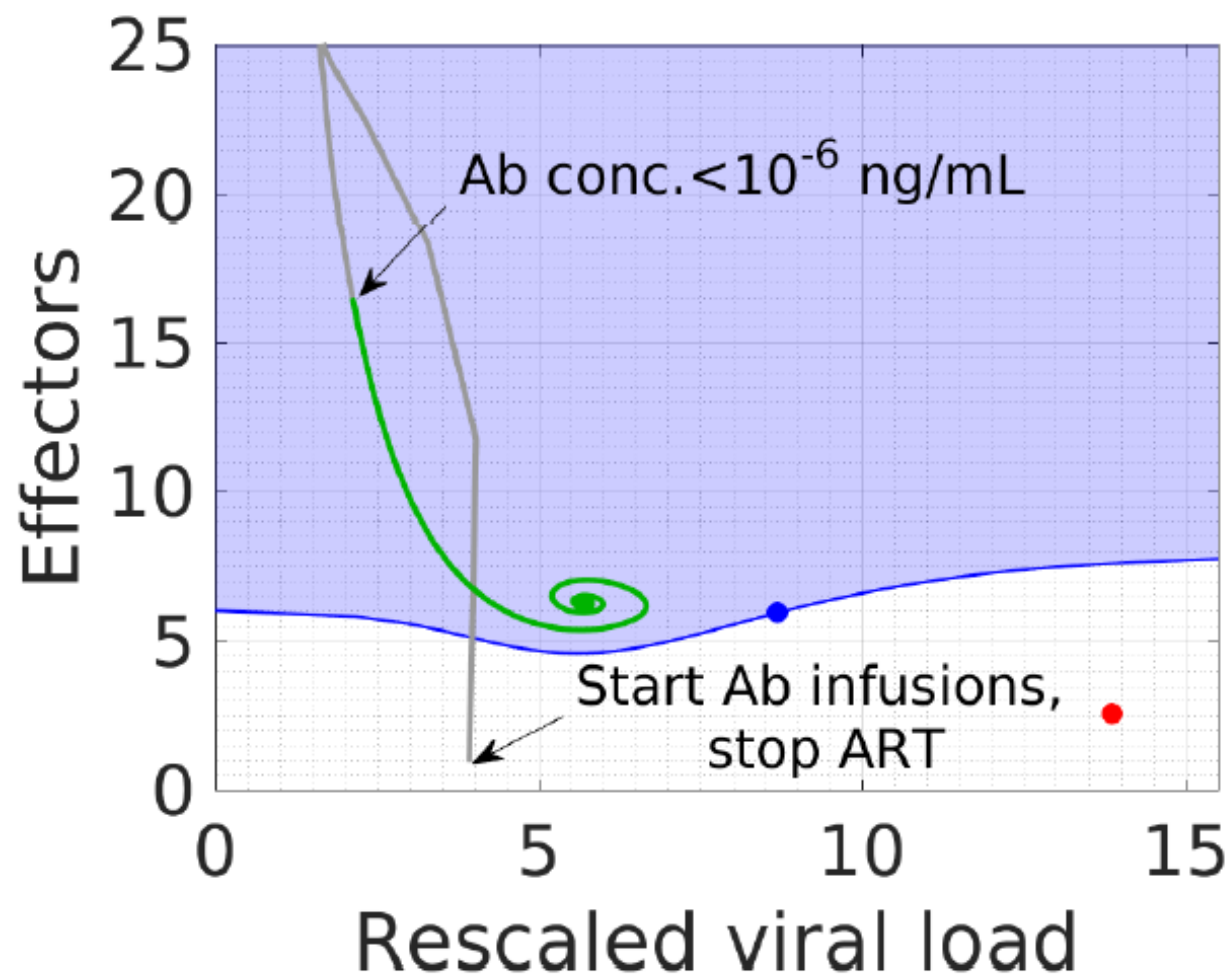
- ▶ Simulate model and track progress of (I, E) from full model simulation on reduced model phase plane.
- ▶ Use P310 parameters with $aL0 = 0.0353$.
- ▶ ATI at day 42.



- ATI at day 44.



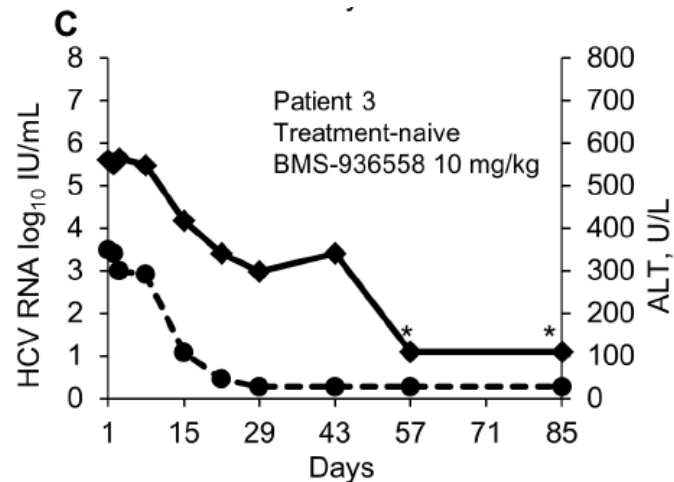
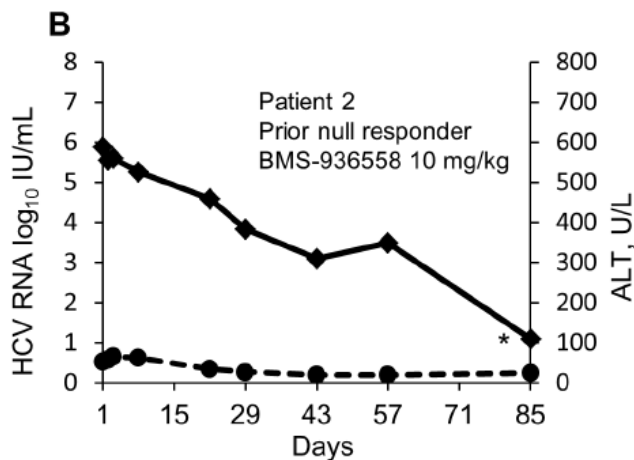
- ▶ ATI at day 0.



Model suggests that infusion of an anti-checkpoint inhibitor, e.g. anti-PD-1 or anti-PD-L1, may be able to convert someone who normally would exhibit viral rebound into a post-treatment controller.

Clinical trials needed to examine this prediction.

One (out of 10) chronically HCV infected patients given a single infusion of anti-PD1 at a dose of 10 mg/kg was cured of infection.



A Randomized, Double-Blind, Placebo-Controlled Assessment of BMS-936558, a Fully Human Monoclonal Antibody to Programmed Death-1 (PD-1), in Patients with Chronic Hepatitis C Virus Infection

David Gardiner^{1*}, Jay Lalezari², Eric Lawitz³, Michael DiMicco⁴, Rheem Ghalib⁵, K. Rajender Reddy⁶, Kyong-Mi Chang^{6,7}, Mark Sulkowski⁸, Steven O' Marro⁹, Jeffrey Anderson¹, Bing He¹, Vikram Kansra^{10a}, Fiona McPhee¹¹, Megan Wind-Rotolo¹⁰, Dennis Grasela¹, Mark Selby¹², Alan J. Korman¹², Israel Lowy¹³